Directional tunnelling spectroscopy of a normal metal-$s+g$-wave superconductor junction

P Pairor†and M F Smith‡

† School of Physics, Institute of Science, Suranaree University of Technology, 111 University Ave., Nakhon Ratchasima, 30000 Thailand
‡ Department of Physics, University of Toronto, 60 St. George St., Toronto, Ontario, M5S 1A7 Canada

E-mail: `pairor@ccs.sut.ac.th`

Abstract. We calculate the normal metal-$s+g$-wave superconductor tunnelling spectrum for various junction orientations. For a junction oriented with its normal parallel to the ab plane of the tetragonal superconductor, we find that the tunnelling spectrum is strongly dependent on orientation in the plane, and contains two peaks at energies equivalent to the magnitudes of the gap function in the direction parallel to the interface normal and in the direction making a $\pi/4$ angle with the normal. These two peaks appear in both superconductors with point nodes and line nodes, but much more prominent in the latter. For the tunnelling along the c axis, there is a sharp peak at the gap maximum in the conductance spectrum of the superconductor with line nodes, whereas in the spectrum of the superconductor with point nodes there is a peak occurring at the value of the gap function along the c axis. We discuss the relevance of our result to borocarbide systems.

Submitted to: *J. Phys.: Condens. Matter*

1. Introduction

Nonmagnetic rare-earth borocarbides, such as YNi_2B_2C and $LuNi_2B_2C$, are among the materials which exhibit unconventional superconductivity. There is strong evidence in these materials indicating that their superconducting gap function is highly anisotropic [1, 2] and that there exist low-lying excitations in the superconducting state [3, 4, 5, 6, 7, 8]. The presence of these low energy excitations implies that the gap function has nodes (or deep minima) on the Fermi surface. The location of these nodes and their nature, i.e., whether they are point nodes or line nodes is still unclear. The thermal conductivity in a magnetic field at low temperatures [1] and the dependence of the specific heat on the magnetic field [3, 6] suggest the existence of the line nodes like those in cuprates and UPt_3. However, the recent measurements of the c axis thermal conductivity in a rotational magnetic field along the ab plane were interpreted as evidence for a gap function with point nodes along [100] and [010] directions [2]. Further studies which employ different experimental techniques may be necessary to determine the detailed structure of the superconducting gap function in momentum space. Here we suggest that directional tunnelling spectroscopy may be useful for this purpose.

In general, the tunnelling conductance spectrum of an anisotropic superconductor is strongly dependent on the crystal orientation with respect to the interface plane. In the case of a d-wave superconductor with vertical line nodes, it has been shown that features in the conductance spectrum occur at voltages which depend strongly on crystal orientation. These voltages correspond to values of the gap function at particular points on the Fermi surface [9]. For instance, in the case of an ab plane tunnelling junction, if the surface orientation of the superconductor is not [100] or [010], the conductance spectrum contains a peak at the voltage corresponding to the value of the gap function in the direction parallel to the surface normal vector. The observation of this feature would, in principle, allow the directional NS tunnelling spectroscopy to map the magnitude of the superconducting gap function.

In this paper, we calculate the normal metal-superconductor (NS) tunnelling spectra of anisotropic s-wave superconductors with two forms of gap functions, which have been suggested as possible candidates for the gap in borocarbides [10, 11]. We find, similar to a d-wave case, that features appear in the spectra at voltages corresponding to values of the gap at particular points on the Fermi surface depending on surface orientation. These features are more prominent in the conductance spectrum of the superconductor that has vertical line nodes than in the spectrum of the superconductor that has point nodes. Thus, if these features can be observed experimentally, it may be possible to determine which form of the gap, if either, correctly describes that of the borocarbides.

The two candidate gap functions are both $s+g$-wave and are given by equation (1a) and (1b) respectively.

$$\Delta_{k,1} = \Delta_s - \Delta_g \cos(4\phi) \tag{1a}$$

$$\Delta_{k,2} = \Delta_s - \Delta_g \sin^2 \theta \cos(4\phi) \tag{1b}$$

where θ and ϕ are the polar angles in spherical coordinates, and Δ_s and Δ_g are the s and g components of the gap function respectively. For an elliptical Fermi surface, the case of line (point) nodes occurs when $\Delta_s = \Delta_g$ in equation (1a) (equation (1b)). We study both ab plane and c axis tunnelling spectra in both cases of the gap function by using the so-called Blonder-Tinkham-Klapwijk (BTK) scattering formalism [12] and a continuous model to describe the electronic structure of the normal metal and superconductor. Although detailed features of the conductance depend on the shape of the Fermi surface, it is sufficient to use the continuous model which gives an elliptical Fermi surface to study the positions of the main features in the conductance spectra [9].

In the case of tunnelling into the ab plane of a $s + g$-wave superconductor, we show in this paper that there are three main features occurring at the voltages associated with the minimum value of the gap function and the values of the gap function in two particular directions with respect to the interface normal: one is in the direction parallel to the surface normal and the other is in the direction making a $\pi/4$ angle with the normal vector. These two features are a lot more prominent for the $s + g$-wave superconductor with line nodes than for the superconductor with point nodes. In the case of c-axis tunnelling junctions, there is one prominent feature at the maximum gap in the conductance spectra of the superconductor with line nodes, whereas for the superconductor with point nodes the conductance spectrum contains two features: one at the maximum gap and the other at the value of the gap function along the c axis.

In the Section 2, we describe the calculation method and the assumptions used throughout this paper. Then, we provide the detailed results and discussions of all the cases of interest at zero temperature in Section 3. In addition to the cases in which the nodes exist, we also consider the cases in which the superconductor is close to having them, i.e., it has nonzero minimum value of the gap function. We show all the results in both the Andreev limit (low barrier) and the tunnelling limit (high barrier).

2. Assumptions and method of calculation

As in reference [12], we represent the NS junction with an infinite system, the left half of which is a normal metal and the right half of which is a superconductor (see figure 1). The insulating barrier is represented by a delta function potential with strength H. For the ab plane tunnelling junctions, the interface normal vector is on the ab plane, and for the c-axis tunnelling junction the normal vector is parallel to the c axis.

We take the normal metal to be cubic, and take the superconductor to be tetragonal to describe the crystal structure of the borocarbides. In our calculation, we ignore both the suppression of the gap function near the NS interface and the proximity effect for simplicity. The gap function Δ_k is taken to be as in either equation (1a) or (1b).

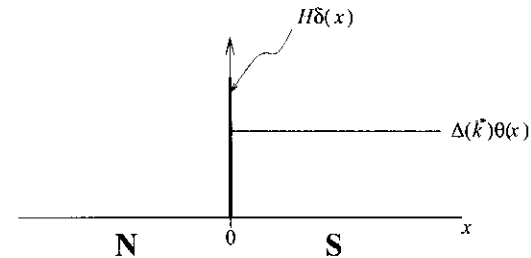The Bogoliubov-de Gennes equations that describe the excitations of the system

Figure 1. The normal metal-superconductor (NS) junction is represented by an infinite system as shown in this picture. The normal metal fills the $x < 0$ region and the superconductor does the $x > 0$ region. The insulator layer is represented by a delta function of height H in units of energy per length. The gap function is taken to be zero on the normal metal and to be nonzero and independent of x in the superconductor.

are

$$\begin{bmatrix} \hat{O}_p + H\delta(x) - \mu & \Delta_k \Theta(x) \\ \Delta_k \Theta(x) & -\hat{O}_p - H\delta(x) + \mu \end{bmatrix} U(\vec{r}) = E U(\vec{r}) \tag{2}$$

where μ is the chemical potential, $\Theta(x)$ is the Heaviside step function,

$$\hat{O}_p = -\frac{\hbar^2}{2} \left(\frac{1}{m_{xy}} \left(\frac{\partial^2}{\partial x^2} + \frac{\partial^2}{\partial y^2} \right) + \frac{1}{m_z} \frac{\partial^2}{\partial z^2} \right),$$

$$m_{xy} = \begin{cases} m \text{ (mass on the normal metal)}, \ x < 0 \\ m_{ab}(ab \text{ plane effective mass of the superconductor}), \ x > 0 \end{cases}$$

$$m_z = \begin{cases} m, \ x < 0 \\ m_c \ (c \text{ axis effective mass of the superconductor}), \ x > 0 \end{cases}$$

and $U(\vec{r})$ is a two-component function:

$$U(\vec{r}) = \begin{bmatrix} u(\vec{r}) \\ v(\vec{r}) \end{bmatrix} = \begin{bmatrix} u_k \\ v_k \end{bmatrix} e^{i\vec{k}\cdot\vec{r}}. \tag{3}$$

After substituting $U(\vec{r})$ from equation (3) into equation(2), we obtain the bulk excitation energies for the normal metal and superconductor respectively as

$$E(\vec{q}) = \pm\xi_q = \pm \left(\frac{\hbar^2}{2m}(q_x^2 + q_y^2 + q_z^2) - \mu \right) \tag{4a}$$

$$E(\vec{k}) = \sqrt{\xi_k^2 + \Delta_k^2} \tag{4b}$$

where for the normal metal (equation (4a))the plus and minus signs are for electron and hole excitations respectively, and for the superconductor (equation (4b))

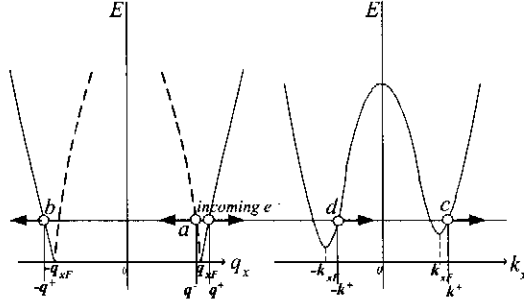$$\xi_k = \frac{\hbar^2}{2} \left(\frac{k_x^2 + k_y^2}{m_{ab}} + \frac{k_z^2}{m_c} \right) - \mu. \tag{5}$$

Figure 2. The plots of excitation energies as a function of q_x or k_x, the component parallel to the interface normal, at a particular value of $\bar{k}_{\parallel}$, which is (k_y, k_z). The plot on the left is for the excitation energy of the normal metal and the plot on the right is for the excitation energy of the superconductor. At the same energy, there can be 4 propagating excitations for each side. However, for an incoming electron from the normal side, the wave function of the normal metal is a linear combination of only 3 excitations represented by the open circles, and the wave function of the superconductor is the sum of 2 outgoing excitations.

Figure 2 shows the plots of the two excitation energies of the normal metal (superconductor) as a function of q_x (k_x), the component along the interface normal vector, at a particular $\vec{q} = \bar{k}_{\parallel} = (k_y, k_z)$, the component perpendicular to the interface normal.

The amplitudes of the excitations, u_k and v_k, of the normal metal are

$$\begin{bmatrix} u_k \\ v_k \end{bmatrix} = \begin{cases} \begin{bmatrix} 1 \\ 0 \end{bmatrix} & \text{for electrons} \\[2ex] \begin{bmatrix} 0 \\ 1 \end{bmatrix} & \text{for holes} \end{cases} \tag{6}$$

whereas those of the superconductor are

$$\begin{bmatrix} u_k \\ v_k \end{bmatrix} = \frac{1}{\sqrt{|E + \xi_k|^2 + \Delta_k}} \begin{bmatrix} \Delta_k \\ E + \xi_k \end{bmatrix}. \tag{7}$$

The wave function of each side is a linear combination of all the appropriate excitations of the same energy and the momentum that has the same component perpendicular to the interface normal. For the tunnelling-into-*ab* plane junction, the wave functions of both sides are therefore

$$U_N(\vec{r}) = \left(\begin{bmatrix} 1 \\ 0 \end{bmatrix} e^{iq^+ x} + a \begin{bmatrix} 0 \\ 1 \end{bmatrix} e^{iq^- x} + b \begin{bmatrix} 1 \\ 0 \end{bmatrix} e^{-iq^+ x} \right) e^{ik_y y + ik_z z} \tag{8a}$$

$$U_S(\vec{r}) = \left(c \begin{bmatrix} u_{k+} \\ v_{k+} \end{bmatrix} e^{ik^+ x} + d \begin{bmatrix} u_{-k-} \\ v_{-k-} \end{bmatrix} e^{-ik^- x} \right) e^{ik_y y + ik_z z} \tag{8b}$$

where $q^{\pm}$ and $k^{\pm}$ (see figure 2) satisfy

$$\hbar q^{\pm} = \sqrt{2m(\mu \pm E) - \hbar^2 k_y^2 - \hbar^2 k_z^2} \tag{9a}$$

$$\frac{\hbar k^{\pm}}{\sqrt{m_{ab}}} = \sqrt{2(\mu \pm \sqrt{E^2 - \Delta_k^2}) - \frac{\hbar^2 k_y^2}{m_{ab}} - \frac{\hbar^2 k_z^2}{m_c}} \tag{9b}$$

and a, b, c, and d are the Andreev reflection, the normal reflection, the same-branched transmission, and the cross-branched transmission amplitudes respectively. For the tunnelling perpendicular to the *ab* plane, or the *c*-axis tunnelling, we can obtain the wave function of each side in a similar way.

Normally, the range of the energy E relevant to the NS tunnelling experiments is of order meV whereas the Fermi energy is of order eV. Therefore, we use the following approximation for q^+ and k^+:

$$q^+ = q^- = \sqrt{\frac{2m\mu}{\hbar^2} - k_y^2 - k_z^2}$$
$$= q_F \sin\theta_N \cos\phi_N \tag{10a}$$

$$k^+ = k^- = k_F \sqrt{\frac{m_{ab}}{m^*}} \sin\theta_S \cos\phi_S \tag{10b}$$

where q_F is the magnitude of the Fermi wave vector of the normal metal, and k_F, m^* are the parameters that satisfy $\hbar^2 k_F^2/(2m^*) = E_{F,S}$, the Fermi energy of the superconductor. Using the conservation of the momentum parallel to the surface, we have the following relationship between the polar angles in spherical coordinates:

$$q_F \sin\theta_N \sin\phi_N = k_F \sqrt{\frac{m_{ab}}{m^*}} \sin\theta_S \sin\phi_S \tag{11a}$$

$$q_F \cos\theta_N = k_F \sqrt{\frac{m_c}{m^*}} \cos\theta_S. \tag{11b}$$

We obtain all the amplitudes a, b, c, and d by applying the following matching conditions at the interface:

$$U_N(x = 0) = U_S(x = 0) \equiv U_0 \tag{12a}$$

$$ZU_0 = \frac{1 + m/m_{ab}}{4k_F} \left(\frac{\partial U_S}{\partial x}\bigg|_{x=0^+} - \frac{\partial U_N}{\partial x}\bigg|_{x=0^-} \right) \tag{12b}$$

where $Z = mH/(\hbar^2 k_F)$. Note that both matching conditions are for the tunnelling-into-*ab*-plane junction. For the *c*-axis tunnelling junction, the first condition remains the same, but we have to replace m_{ab} with m_c in the second condition.

In the BTK formalism, the Andreev reflection, the normal reflection, and the two transmission probabilities are used to obtain the current across the junction. All the reflection and transmission probabilities are obtained from

$$A = |a|^2 \left(\frac{q^-}{q^+} \right) \tag{13a}$$

$$B = |b|^2 \tag{13b}$$

$$C = |c|^2 \left(|u_{k+}|^2 - |v_{k+}|^2\right)\left(\frac{k^+}{q^+}\right) \tag{13c}$$

$$D = |d|^2 \left(|u_{-k}|^2 - |v_{-k}|^2\right)\left(\frac{k^-}{q^+}\right) \tag{13d}$$

and satisfy: $A + B + C + D = 1$, i.e., the number of particles is conserved.

On the normal metal side, we find the current across the junction as a function of an applied voltage is

$$I_{NS}(V) = \frac{e\Omega}{(2\pi)^3}\int d\vec{q}\, v_{q_x}[1 + A(\vec{q}) - B(\vec{q})][f(E_q - eV) - f(E_q)] \tag{14}$$

where Ω is volume, v_{q_x} is the group velocity of the incoming electron, and $f(E)$ is the Fermi-Dirac distribution function.

The conductance of the ab plane junction at zero temperature thus becomes

$$G_{NS}^{ab}(V) = \frac{dI_{NS}^{ab}}{dV}$$
$$= \frac{me^3\Omega V}{4\pi^2\hbar^2}\int d\phi_N \int d\theta_N \sin^2\theta_N \cos\phi_N[1 + A(V,\phi_N,\theta_N) - B(V,\phi_N,\theta_N)] \tag{15}$$

Similarly, the conductance of the c-axis junction is

$$G_{NS}^{c}(V) = \frac{me^3\Omega V}{4\pi^2\hbar^2}\int d\phi_N \int d\theta_N \sin\theta_N \cos\theta_N[1 + A(V,\phi_N,\theta_N) - B(V,\phi_N,\theta_N)] \tag{16}$$

The limits of both integrals can be found by considering equation(11a) and (11b).

3. Results and discussions

We plot the normalized conductance as a function of applied voltage of both ab plane and c axis tunnelling. We define the normalized conductance as the conductance of the junction normalized with its value at a high voltage, i.e., $eV \gg \Delta_{max}$, the maximum magnitude of the gap function. Using both forms of the gap function in equation(1a) and (1b), we consider 3 cases:(1) $\Delta_s = \Delta_g$, (2) $\Delta_s = 0.9\Delta_g$, and (3) $\Delta_s = 1.1\Delta_g$. These choices are in accordance with the fact that the gap anisotropy of at least a factor of 10 as suggested by thermal conductivity measurements [1]. All the results are obtain for zero temperature.

3.1. ab plane tunnelling

Figure 3 shows the diagram of the junction that has the interface normal on the ab plane of the superconductor. We specify the orientation in the ab plane with α, the angle between the interface normal and the a axis of the superconductor. The gap function is now a function of α,

$$\Delta_{k+,1} = \Delta_s - \Delta_g \cos 4(\phi_S \mp \alpha) \tag{17a}$$

$$\Delta_{k\pm,2} = \Delta_s - \Delta_g \sin^2\theta_S \cos 4(\phi_S \mp \alpha) \tag{17b}$$

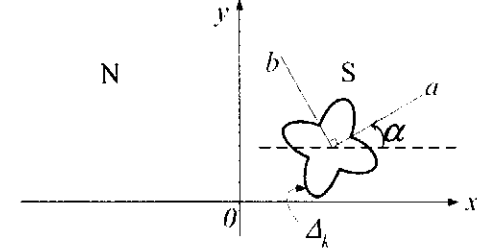**Figure 3.** The geometry of the ab plane tunnelling NS junction. The angle between the x axis and the a axis, α, defines the orientation of the junction.

In the Andreev limit (small Z), the conductance spectrum depends very little on the junction orientation. As shown in figure 4 for $\Delta_{k,1}$ and figure 5 for $\Delta_{k,2}$, the conductance spectra in all cases have the inverted gap structure. Note that in the case of $\Delta_{k,2}$ in figure 5, there is a slight kink at the voltage associated with the value of the gap function along the c axis (eV $= 0.5\Delta_{max}$). Also note that when $\Delta_s \neq \Delta_g$, there is a feature occurring at $eV = |\Delta_s - \Delta_g|$ as marked by the arrows in figure 4 (b),(c) and figure 5 (b),(c).

In the tunnelling limit (large Z), the shape of the conductance spectrum changes with the interface orientation. First, consider the case where $\Delta_s = \Delta_g$, there are two distinct peaks, which are more pronounced for the superconductor with the gap function $\Delta_{k,1}$ than for the superconductor with the gap function $\Delta_{k,2}$ (compare figure 6 (a) and figure 7 (a)). The two peaks occur at the voltages corresponding to $\Delta_{k,i}(\theta, \phi = 0, \alpha)$ (marked by the filled arrows) and $\Delta_{k,i}(\theta, \phi = \pi/4, \alpha)$ (marked by the hollowed arrows), where i is either 1 or 2. Notice that when $\alpha = \pi/8$, there is only one peak due to the fact that $\Delta_{k,i}(\theta, \phi = 0, \alpha = \pi/8) = \Delta_{k,i}(\theta, \phi = \pi/4, \alpha = \pi/8)$.

In the case of $\Delta_s = 0.9\Delta_g$, $\Delta_{k,i}$ can be both positive and negative. Consequently, for the orientations with $\alpha \neq 0, \pi/4$, in addition to the two peaks like in the case of $\Delta_s = \Delta_g$, there exists a peak at zero voltage (figure 6 (b) and 7 (b)). The existence of this zero-bias conductance peak, which also occurs in the d-wave case, is a signature of the presence of a sign change of the gap function [13, 14].

When $\Delta_s = 1.1\Delta_g$, there is a finite gap minimum. The conductance is very small for voltages less than the gap minimum, and the two peaks at $\Delta_{k,i}(\theta, \phi = 0, \alpha)$ and $\Delta_{k,i}(\theta, \phi = \pi/4, \alpha)$ are still present.

In summary, the conductance spectrum in every case where $\alpha \neq 0, \pi/4$ contain the two peaks at $\Delta_{k,i}(\theta, \phi = 0, \alpha)$ and $\Delta_{k,i}(\theta, \phi = \pi/4, \alpha)$. These two angles, $\phi = 0, \pi/4$, are special because the magnitude of the gap function of the two transmitted superconducting excitations with the k_y corresponding to these angles is the same,
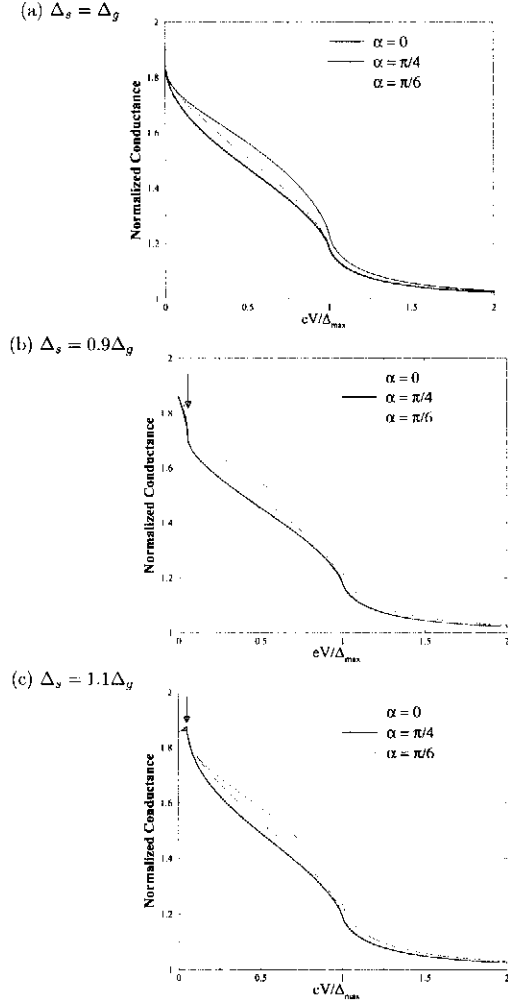
(a) $\Delta_s = \Delta_g$

(b) $\Delta_s = 0.9\Delta_g$

(c) $\Delta_s = 1.1\Delta_g$

Figure 4. *ab plane tunnelling junctions.* The plots of the $Z = 0.0$ normalized conductance spectra for 3 surface orientations in 3 cases of the gap function $\Delta_{k\pm,1} = \Delta_s - \Delta_g \cos 4(\phi_S \mp \alpha)$, i.e., (a) $\Delta_s = \Delta_g$, (b) $\Delta_s = 0.9\Delta_g$, and (c) $\Delta_s = 1.1\Delta_g$. The arrows in (b) and (c) point at the feature occurring at voltage corresponding to $|\Delta_s - \Delta_g|$.
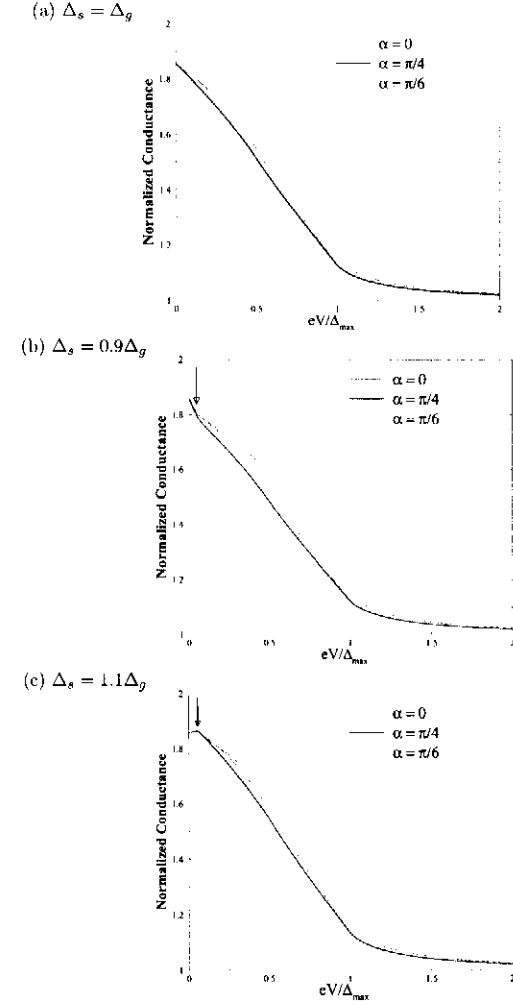
(a) $\Delta_s = \Delta_g$

(b) $\Delta_s = 0.9\Delta_g$

(c) $\Delta_s = 1.1\Delta_g$

Figure 5. *ab plane tunnelling junctions.* The plots of the $Z = 0.0$ normalized conductance spectra for 3 surface orientations in 3 cases of the gap function $\Delta_{k\pm,2} = \Delta_s - \Delta_g \sin^2 \theta_S \cos 4(\phi_S \mp \alpha)$, i.e., (a) $\Delta_s = \Delta_g$, (b) $\Delta_s = 0.9\Delta_g$, and (c) $\Delta_s = 1.1\Delta_g$. The arrows in (b) and (c) point at the feature occurring at voltage corresponding to $|\Delta_s - \Delta_g|$.
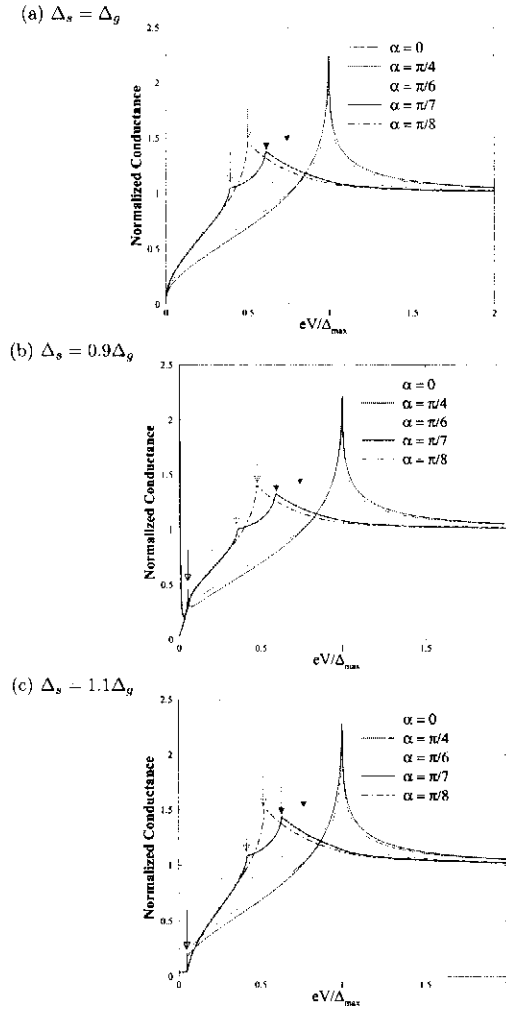
(a) $\Delta_s = \Delta_g$

(b) $\Delta_s = 0.9\Delta_g$

(c) $\Delta_s = 1.1\Delta_g$

Figure 6. *ab plane tunnelling junctions.* The plots of the $Z = 3.0$ normalized conductance spectra for 3 interface orientations in 3 cases of the gap function $\Delta_{k^\pm,1} = \Delta_s - \Delta_g \cos 4(\phi_S \mp \alpha)$, i.e., (a) $\Delta_s = \Delta_g$, (b) $\Delta_s = 0.9\Delta_g$, and (c) $\Delta_s = 1.1\Delta_g$. The hollowed arrows point at the features occurring at voltage corresponding to $\Delta_{k,1}(\theta = 0, \phi = \pi/4, \alpha)$ and the filled arrows point at voltage corresponding to $\Delta_{k,1}(\theta = 0, \phi = 0, \alpha)$.
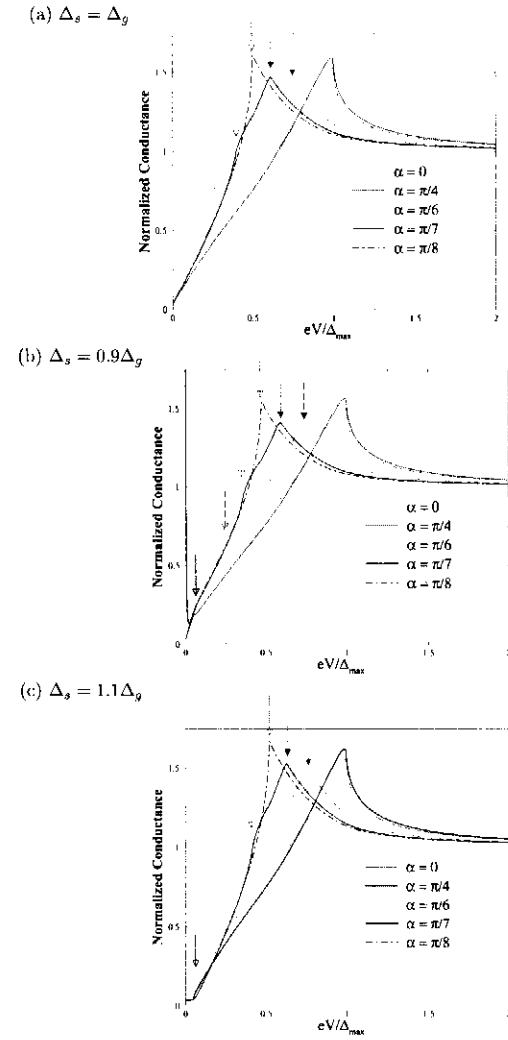
(a) $\Delta_s = \Delta_g$

(b) $\Delta_s = 0.9\Delta_g$

(c) $\Delta_s = 1.1\Delta_g$

Figure 7. *ab plane tunnelling junctions.* The plots of the $Z = 3.0$ normalized conductance spectra for 3 interface orientations in 3 cases of the gap function $\Delta_{k^\pm,2} = \Delta_s - \Delta_g \sin^2 \theta_S \cos 4(\phi_S \mp \alpha)$, i.e., (a) $\Delta_s = \Delta_g$, (b) $\Delta_s = 0.9\Delta_g$, and (c) $\Delta_s = 1.1\Delta_g$. The hollowed arrows point at the features at voltage corresponding to $\Delta_{k,2}(\theta = 0, \phi = \pi/4, \alpha)$ and the filled arrows point at voltage corresponding to $\Delta_{k,2}(\theta = 0, \phi = 0, \alpha)$.
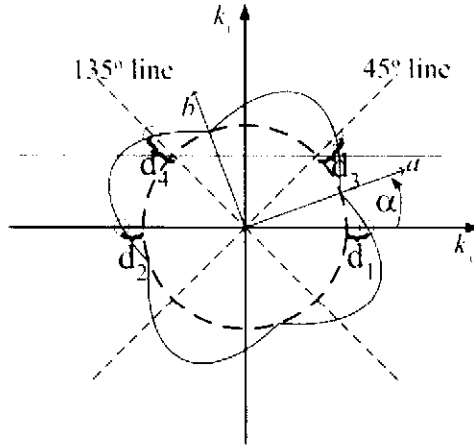
Figure 8. This picture shows the gap function in the momentum space, when $\alpha \neq 0, \pi/4$. The dashed circle is the contour of the Fermi surface projected on the $k_x k_y$ plane. The solid curve represents the gap function. The two dashed lines are the $\phi = \pi/4$ and $\phi = 3\pi/4$ lines. The solid horizontal line above $k_y = 0$ is the line of constant $k_y = k_y(\phi = \pi/4)$ on the Fermi surface. Note that $d_1 = d_2$ (the magnitude of the gap when $\phi = 0$) and $d_3 = d_4$ (the magnitude of the gap when $\phi = \pi/4$).

i.e., $\Delta_{k^+} = \Delta_{k^-}$ only when $\phi = 0, \pi/4$, as shown pictorially in figure 8. We should also emphasize that the two peaks at $\Delta_{k,i}(\theta, \phi = 0, \alpha)$ and $\Delta_{k,i}(\theta, \phi = \pi/4, \alpha)$ are more prominent for the superconductor with the gap function $\Delta_{k,1}$ than for the superconductor with the gap function $\Delta_{k,2}$. Even though this finding may not aid in distinguishing the tunnelling spectra of superconductors with line nodes and point nodes, we can use it to determine the magnitude of the gap function in a particular direction directly.

3.2. c-axis tunnelling

Because in the continuous model the Fermi surface of a tetragonal crystal is invariant under rotation around the c-axis of the crystal, the c axis tunnelling spectroscopy is independent of the rotation around the c axis. In the Andreev limit, when $|\Delta_s - \Delta_g| < eV < \Delta_{max}$, the conductance curve of the superconductor with line nodes is downward and decreasing smoothly (see figure 9 for $Z = 0$). On the contrary, the conductance curve of the superconductor with point nodes is upward when $|\Delta_s - \Delta_g| < eV < 0.5\Delta_{max}$ is downward (see figure 10 for $Z = 0$). The value $0.5\Delta_{max}$ is the magnitude of the gap along c axis.
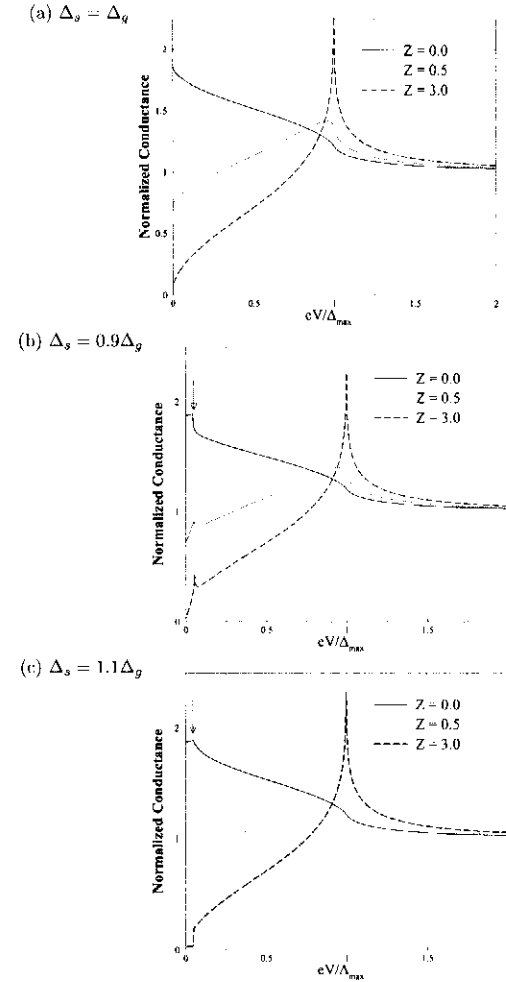
(a) $\Delta_s = \Delta_g$

(b) $\Delta_s = 0.9\Delta_g$

(c) $\Delta_s = 1.1\Delta_g$

Figure 9. *c- axis tunnelling junctions.* The plots of the normalized conductance spectra for different values of Z in 3 cases of the gap $\Delta_{k,1} = \Delta_s - \Delta_g \cos 4(\phi_S + \alpha)$:(a) $\Delta_s = \Delta_g$, (b) $\Delta_s = 0.9\Delta_g$, and (c) $\Delta_s = 1.1\Delta_g$. The arrows are pointing at a feature occurring at $|\Delta_s - \Delta_g|$.
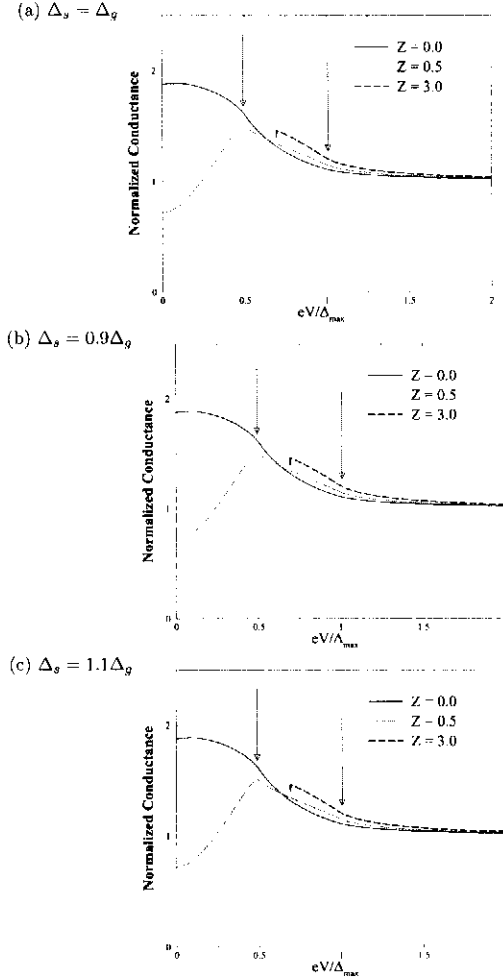
(a) $\Delta_s = \Delta_g$

(b) $\Delta_s = 0.9\Delta_g$

(c) $\Delta_s = 1.1\Delta_g$

Figure 10. *c- axis tunnelling junctions.* The plots of the normalized conductance spectra for different values of Z in three cases of the gap $\Delta_{k,2} = \Delta_s - \Delta_S \sin^2 \theta_S \cos 4(\phi_S \mp \alpha)$:(a) $\Delta_s = \Delta_g$, (b) $\Delta_s = 0.9\Delta_g$, and (c) $\Delta_s = 1.1\Delta_g$. The arrows are pointing at features occurring at $\Delta_{k,2}(\theta_S = 0)$ and the maximum gap.

In the tunnelling limit, the spectrum of the superconductor with the gap function $\Delta_{k,1}$ contains a peak at the gap maximum and a feature at eV $= |\Delta_s - \Delta_d|$ (see figure 9 for $Z = 3.0$. The spectrum of the superconductor with the gap function $\Delta_{k,2}$ contains two features at eV $= |\Delta_s - \Delta_g|$ and the gap maximum, and a sharp peak at $\Delta_{k,2}(\theta = 0)$, the value of the gap function along the c axis (see figure 10 for $Z = 3$). The occurrence of the peak at different positions in the conductance spectrum enable us to distinguish the tunnelling spectrum of a line-node superconductor and a point-node superconductor.

4. Conclusions

We have studied the c-axis and ab plane tunnelling spectroscopy of $s + g$-wave superconductors. The observation of the features in tunnelling measurements made for various junction orientations would, in principle, provide a way to study the detailed momentum dependence of an $s+g$-wave superconducting gap. In borocarbides, the gap function of which has been suggested to be $s+g$-wave with either line or point nodes, tunnelling spectroscopy would help to determine whether either form of the superconducting gap is correct. The c-axis tunnelling spectra of a superconductor with line nodes and a superconductor with point nodes are distinguishable. In the tunnelling limit, the c axis tunnelling conductance spectrum of a line-node superconductor contains a sharp peak at the gap maximum, whereas in the spectrum of of a point-node superconductor the sharp peak is at the value of the gap function along the c axis.

The ab plane tunnelling spectra of the two cases of nodes are not as distinguishable as the c-axis spectra; however, they can be used to map out the magnitude of the gap function on the plane. The conductance spectrum of ab plane tunnelling junction is strongly dependent on the junction orientation. Two features in the spectrum appear at energies equal to the magnitude of the superconducting gap in two momentum directions: one is the direction parallel to the interface normal and the other is the direction making a $\pi/4$ angle with the interface normal. It is worth noted that these features are more prominent in the spectrum of the superconductor with line nodes than in the spectrum of the superconductor with point nodes, although this prominence may not be distinguishable especially at finite temperatures. The feature at the gap in the direction parallel to the interface normal has been shown to occur in a d-wave superconductor as well [9]. However, the feature at the gap in the direction making a $\pi/4$ angle with the interface normal is unique to an anisotropic s-wave superconductor. This uniqueness is due to the fact that the gap function of an anisotropic s-wave superconductor always has the same sign, unlike in a d-wave case in which the values of the gap of the two outgoing excitations with $\phi_S = \pi/4$ always have different sign for all junction orientations except [100] and [010] junctions. This sign difference results in a zero-bias conductance peak in a d-wave case, instead of a peak at energies equivalent to the gap in the $\pi/4$ direction.

Acknowledgments

[1] Etienne Boaknin *et al* 2001 Phys. Rev. Lett. **87** 237001
[2] K. Izawa *et al* 2002 Phys. Rev. Lett. **89** 137006
[3] K. Izawa *et al* 2001 Phys. Rev. Lett. **86** 1327
[4] T. Jacobs *et al* 1995 Phys. Rev. B **52** 007022
[5] In-Sang Yang *et al* 2000 Phys. Rev. B **62** 1291
[6] M. Nohara *et al* 1999 J. Phys. Soc. Jpn. **68** 1078
[7] M. Nohara *et al* 2000 Physica (Amsterdam) **341C-348C** 2177
[8] M. Nohara *et al* 1997 J. Phys. Soc. Jpn. **66** 1888
[9] P. Pairor and M. B. Walker 2002 Phys. Rev. B **65** 064507
[10] K. Maki *et al* 2002 Phys. Rev.B **65** 140502
[11] Hyun C. Lee and Han-Yong Choi 2002 Phys.Rev. B **65** 174530
[12] G. E. Blonder *et al* 1982 Phys. Rev. B **25** 004515
[13] C.-R. Hu 1994 Phys. Rev. Lett. **72** 001526
[14] S. Kashiwaya *et al* 1996 Phys. Rev. B **53** 002667

หนึ่งผลงานหนึ่งอาจารย์ (อ. ดร. พวงรัตน์ ไพเราะ สาขาวิชาฟิสิกส์ สำนักวิชาวิทยาศาสตร์)

หัวข้อที่เสนอ   การศึกษา Tunnelling spectroscopy of MgB_2

ผลงานคาดหวัง งานตีพิมพ์ 1 ฉบับ

ผลงานที่ได้   ผลงานเรื่อง Directional tunnelling spectroscopy of a normal metal- $s+g$-wave superconductor junction ส่งตีพิมพ์ ในวารสาร Journal of Physics: Condensed Matter (โปรดดูเอกสารแนบ ซึ่งเป็น preprint)